



**HAL**  
open science

## Exploratory study to define new observation geometries for road lighting design

Laure Lebouc, Florian Greffier, Vincent Boucher, Aurélia Nicolaï, Paul  
Richard

### ► To cite this version:

Laure Lebouc, Florian Greffier, Vincent Boucher, Aurélia Nicolaï, Paul Richard. Exploratory study to define new observation geometries for road lighting design. *International Journal of Lighting Research and Technology*, 2024, 10.1177/14771535241265720 . hal-04671426

**HAL Id: hal-04671426**

**<https://hal.science/hal-04671426v1>**

Submitted on 10 Feb 2025

**HAL** is a multi-disciplinary open access archive for the deposit and dissemination of scientific research documents, whether they are published or not. The documents may come from teaching and research institutions in France or abroad, or from public or private research centers.

L'archive ouverte pluridisciplinaire **HAL**, est destinée au dépôt et à la diffusion de documents scientifiques de niveau recherche, publiés ou non, émanant des établissements d'enseignement et de recherche français ou étrangers, des laboratoires publics ou privés.

# Exploratory study to define new observation geometries for road lighting design

L Lebouc<sup>1</sup>, F Greffier<sup>1</sup>, V Boucher<sup>1</sup>, A Nicolai<sup>2</sup>, P Richard<sup>3</sup>

<sup>1</sup> Cerema, Les Ponts-de-Cé, France

<sup>2</sup> Spie Batignolles Malet, Portet-sur-Garonne, France

<sup>3</sup> LARIS - SFR MATHSTIC, Université d'Angers, Angers, France

Short title: Exploratory study to define new observation geometries

Received 24 January 2024; Revised 22 May 2024; **Accepted**

This article focuses on the visibility of road users in urban environment. First, a virtual reality experiment was carried out to determine where road users look on the road surface when travelling in city. The data collected were used to deduce observation angles for each type of road user. Measurements on an experimental site and simulations were carried out with these new observation angles. These were used to assess the impact of changing the observation geometry on the quality criteria of a lighting installation and on the visibility criterion. The results show that increasing the observation angle leads to a reduction in the average luminance but that, despite this, visibility is not affected. This led us to propose adaptations to the current recommendations: using a mobile observer for an observation angle greater than 1° and downgrading by one class when dimensioning a lighting installation in the city in the standard way, while taking into account the visual needs in an urban environment.

Address for correspondence: Laure Lebouc, Cerema - Site d'Angers, 23 Avenue de l'Amiral Chauvin, 49130 Les Ponts-de-Cé, France. E-mail: laure.lebouc@cerema.fr

## **1 Introduction**

Performance requirements for road and tunnel lighting are defined in CIE (International Commission on Illumination) or CEN (European Committee for Standardization) documents.<sup>1-4</sup> These standards specify performance criteria based on the average luminance of the road surface, the overall and longitudinal uniformities of lighting to satisfy the visual needs of users. They also describe the methodology for calculating these criteria when designing an installation or for measuring them on site.

These criteria are defined for only one observation geometry. It considers user's eyes at 1.50 m above the road surface with a line of sight at 1° below the horizontal. This geometry is still recommended for a motorist travelling on an interurban road at a speed of between 70 and 90 km/h. However, most street lighting today is located in urban areas, where the average speed is between 30 and 50 km/h. Furthermore, urban lighting must meet the visual needs of all users of public space to ensure the highest possible safety and comfort. This applies not only to motorists but also to cyclists and pedestrians. More and more studies<sup>5-8</sup> are therefore currently aimed at reconsidering standard geometry to define new ones, more adapted to the urban environment and to the diversity of users. As Muzet *et al.*<sup>7</sup> suggest, it is important for road safety to have good visibility of obstacles beyond the stopping distance. This can already give an idea of the minimum angles of observation required for each type of user.

Our study is therefore conducted in two steps. First, in order to identify the need for light on road surfaces, it is essential to know where users are looking on the ground in order to provide them with the right amount of light, the light they need to travel safely. For this, virtual reality techniques coupled with eye-tracking are used to study the influence of the travel modality (pedestrian, cyclist, motorist) on the observation angle in a night-time urban environment. Secondly, based on the results obtained, the evolution of the road lighting performance criteria and the visibility level of a target according to the change of observation angle is studied.

## **2 Where do users look when they travel at night?**

### **2.1 Method**

Forty-five people participated in the experiment (38 males and 7 females, aged 15 y to 61 y; of whom 22% in the 15-29 age group, 53% in the 30-49 age group and 25% in the 50+ age group). Data from eight participants were excluded from the analysis because they did not complete the experiment due to kinetosis. All participants gave their verbal consent to take part in the research.

They were equipped with a virtual reality headset (VIVE Pro Eye manufactured by HTC) which included an eye-tracking system and headphones. The virtual reality headset was connected

to a computer on which it was possible to see what the participant was looking at in real time and track their progress through the virtual world. A joystick connected to the computer allowed participants to navigate around the virtual city.

The virtual environment was designed with Unity 3D. The simulated scene takes place at night and represents a city consisting of several streets with an interurban road around it (see Figure 1). This interurban road consists of four straight sections of about 1800 m each and four curves. Only pedestrians were present in the city: there was no other ambient traffic to ensure a repeatable driving scene for all subjects. A moving camera was used to symbolize the user's field of view. It was placed 1.5 m above the road surface to match road lighting standards.<sup>2</sup>

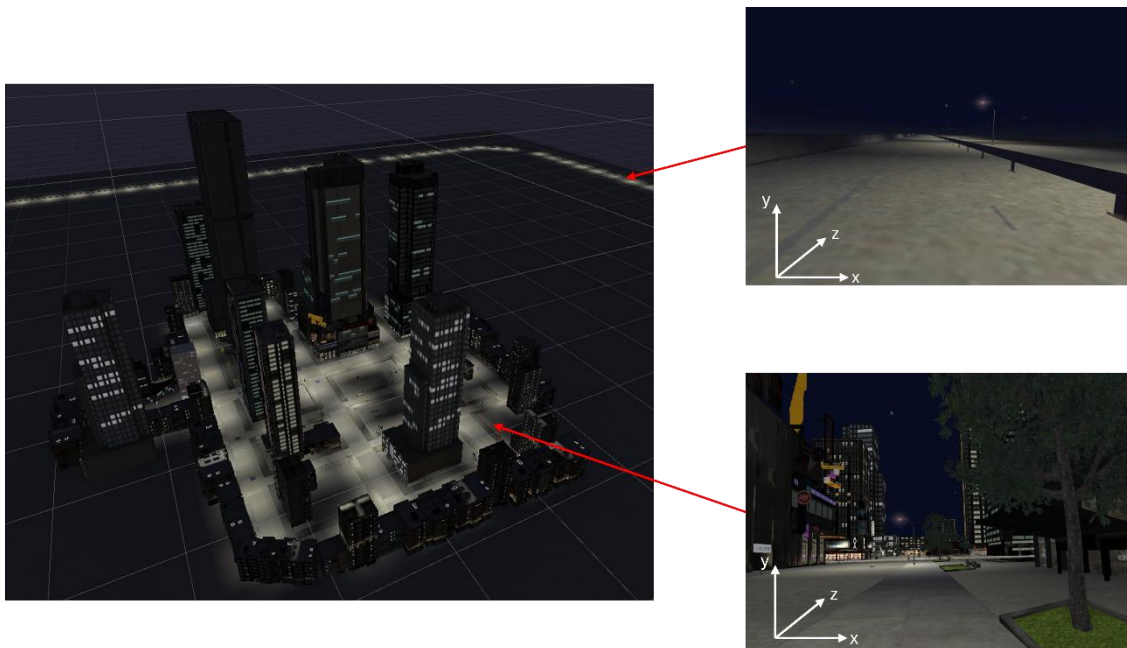


**Figure 1** – On the left, top view under Unity of the virtual environment (city and portion of bypass in the background). On the right, examples of visuals of a city street at the bottom and a portion of the interurban road at the top

Participants were asked to follow audible instructions and to focus on their path, *i.e.* the road or the sidewalk, in the same way as in a real situation. They also had to signal, with a button on the gamepad, the presence of an obstacle represented by a red half-sphere, as soon as they saw it, to ensure the simultaneous dual task. These appearances were programmed to occur at random intervals between 20 and 40 s at a random distance from the camera in the virtual world between 25 and 60 m. The stimulus appeared at ground level, in the direction of the participant's gaze. For each appearance, the obstacle remained visible for 5 s and then disappeared.

Each participant completed a run for each of the four travel modalities (pedestrian, cyclist, urban motorist, and intercity motorist) in a random order. Each run lasted 300 s. For each

travel modality, participants all travelled the same route. However, a different route was associated with each travel mode so that knowledge of the route did not influence the results for another mode. The speed of travel was 6 km/h for pedestrians, 12 km/h for cyclists, 25 km/h for motorists in town and 75 km/h for motorists on interurban roads. At the end of each experiment, the resulting file contained the following information:

- time stamp,
- the participant's mode of travel (pedestrian, cyclist, city or intercity motorist),
- the reaction time to detect the red half-spheres,
- the coordinates  $x_{cam}, y_{cam}, z_{cam}$  of the participant in the virtual world,
- the coordinates  $x_{impact}, y_{impact}, z_{impact}$  of the intersection of the gaze with the object in the virtual world (cf. Figure 2),
- the name of the object examined (road, building, urban furniture, etc.).

This information was recorded during the experiment at a frequency of 20 Hz (every 0.05 s).

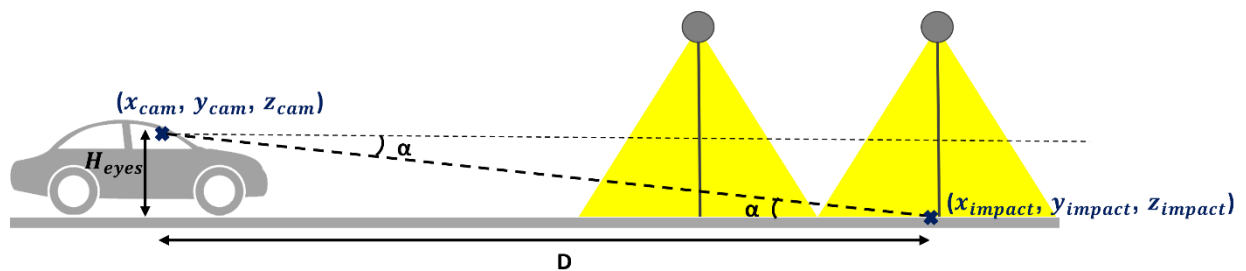


**Figure 2** – Illustration of the different coordinates in the virtual world

## 2.2 Results

### 2.2.1 Data processing

For each participant, the recorded data were retrieved (a total of 24,000 eye-tracking data per person) and separated them according to the travel mode (6,000 per modality per person). The reaction times of the participants were observed to see if they were complying with the given instruction (focus on the route). Delayed responses were used to identify moments when attention was diverted. None of the participants was excluded. However, it was decided not to include the first 100 observations of each individual for each travel mode (*i.e.* the first 5 seconds for each trip) in the treatments because this was the average time it took for participants to start moving at the beginning of each run.

Then, since the road surface (the street or the sidewalk) is the most important element of the visual field for user's movement,<sup>2,9</sup> the oculometric data are filtered to keep only those corresponding to looking at this road surface. The observations of all participants validating this condition are then grouped. Observation angles  $\alpha$  are then derived from Equation 1. Unity

uses a left-hand coordinate system such that  $x$  and  $z$  coordinates define the ground plane and  $y$  is oriented upward (Figure 1).

$$\alpha = \cos^{-1} \left( \frac{\sqrt{(x_{impact} - x_{cam})^2 + (z_{impact} - z_{cam})^2}}{\sqrt{(x_{impact} - x_{cam})^2 + (y_{impact} - y_{cam})^2 + (z_{impact} - z_{cam})^2}} \right) \quad (1)$$

Box plots<sup>10</sup> of the calculated angles  $\alpha$  for each travel modality are then drawn. Since an average observation angle is sought based on the travel modality, data beyond the boundaries of the whiskers are removed to eliminate outliers. Thus, for each modality, angles that are not in the range  $[Q1 - 1.5 \times IQR; Q3 + 1.5 \times IQR]$  have been excluded, where  $Q1$  is the 25<sup>th</sup> quantile,  $Q3$  is the 75<sup>th</sup> quantile, and  $IQR$  is the interquartile range of the given distribution. The box plots of the calculated angles for each travel modality are then plotted in Figure 3.

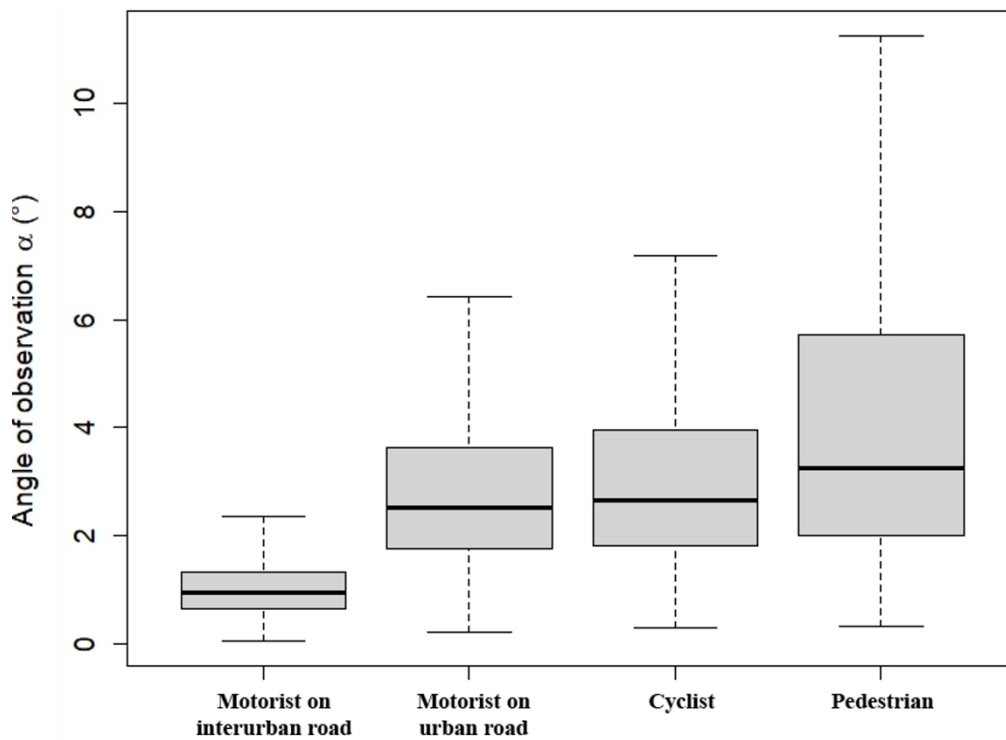


**Figure 3** – The distribution of observation angles for each travel modality

### 2.2.2 Analysis and results

Figure 3 shows the distributions of observation angles obtained for each travel mode. These distributions do not follow normal laws according to the Kolmogorov-Smirnov test<sup>10</sup> (for all distributions,  $p < 0.05$ ). Therefore, statistical analyses were performed using non-parametric difference tests. The Friedman test<sup>10</sup> was used to compare travel modes because the samples compared were dependent (same participants for all modalities). As the samples were not all

of the same size, cells of  $0.1^\circ$  were used to plot the probability distributions of the observation angles for all the modalities (Figure 4). Friedman's test was then carried out for each mode of travel using the probabilities of each cell. The results of this test show that the distributions of observation angles are statistically different ( $p < 0.05$ ). Table 1 summarises the average observation angle and its standard deviation (Equations 2 and 3), the distance  $D$  in the road plane corresponding to this average angle (Figure 2), and the average reaction time to obstacle detection and its standard deviation.

$$\alpha_{mean} = \sum_i \alpha_i \times p(\alpha_i) \quad (2)$$

$$\sigma = \sqrt{\left(\sum_i \alpha_i^2 \times p(\alpha_i)\right) - \left(\sum_i \alpha_i \times p(\alpha_i)\right)^2} \quad (3)$$

where  $p(\alpha_i)$  is the probability of occurrence of the observation angle  $\alpha_i$ .

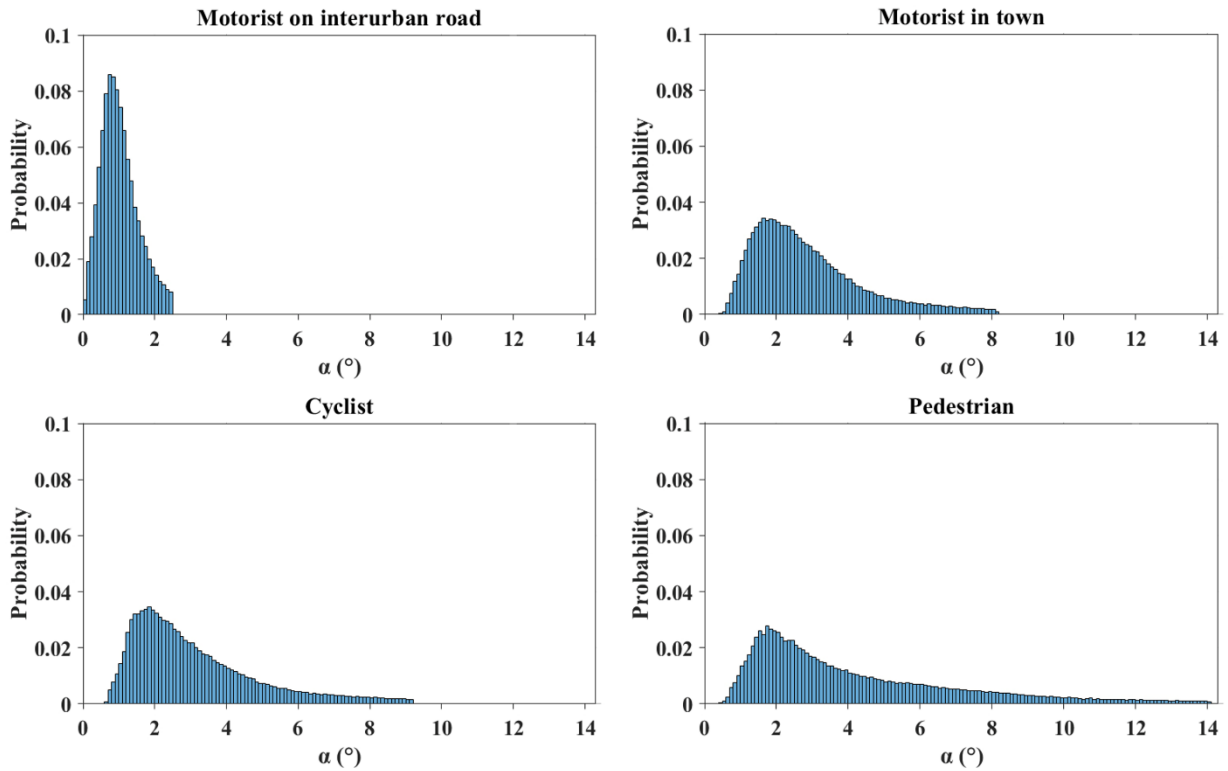


**Figure 4** – Probability distributions of observation angles  $\alpha$  for each of the four travel modes.

## 2.3 Discussion

First of all, it can be noticed that an average angle equal to  $1^\circ$  for motorists in interurban areas was found, which is the standard angle defined for the dimensioning of road lighting.<sup>2</sup> This result indicates a good scaling of the virtual environment and gives confidence in the implementation of the experimentation. Moreover, the results suggest that there is a significant effect of the travel mode on the distance at which the observer looks. It can be seen that the average observation angle varies from  $1.0^\circ$  for a car driver in interurban areas to  $4.2^\circ$  for a pedestrian in the city. This corresponds to looking at a distance of around 86 m for the interurban driver and decreases to a distance of 20 m for the pedestrian. This can be explained by the speed of travel and the necessary anticipation to detect possible obstacles on the road or sidewalk. As our travel speed increases, we need a greater distance to stop<sup>7</sup> and therefore need to look far away to anticipate this possible stop (Table 1). This could partly explain the gap in distance between city users and interurban motorists. Furthermore, the average observation angles for a cyclist ( $3.1^\circ$ ) and a motorist in the city ( $2.9^\circ$ ) are close but significantly different in terms of the statistical test.<sup>10</sup>

The second result is found in the distribution of the data. Indeed, when the dispersion of the angles obtained for each travel mode is observed in Figure 4, it can be seen that city users tend to scan more the road surface in front of them, particularly pedestrians (angles up to about  $14^\circ$  below the horizontal), whereas a car driver on an interurban road will not look closer than about 34 m in front of him (maximum angle equal to  $2.5^\circ$ ). This result is confirmed by the observation of the standard deviations of the observation angles, which increase as the speed decreases (see Table 1). Furthermore, when the average reaction time of the participants for each travel mode is calculated, it appears that the reaction time to the visual stimulus decreases as the speed increases (see Table 1). This is consistent with the previous results since as our speed increases, our attentional field of view decreases and our gaze is distributed in a narrow range of viewing angles. Thus, our attention is focused on a smaller area and when a visual stimulus appears in this area, our reaction time is shorter. In addition, the size of the visual stimulus increases more rapidly in the visual field for faster modes of travel, making it easier to detect.

## 3 New observation geometries

We now know that, depending on their mode of travel, users do not look at the same distance ahead. But does this have an impact on the performance criteria for lighting installations?

In order to study the impact of a change in observation geometry, it was decided to evaluate the performance of a lighting installation for different types of users by simulation and by measurement on an experimental site. An angle  $\alpha$  of  $1^\circ$  is maintained for motorists on interurban roads. Then, an observation angle equal to  $3^\circ$  is assigned for motorists in city and cyclists, an angle that has also been proposed by Stockmar.<sup>8</sup> Finally, following the  $2^\circ$



increment, an  $\alpha$  angle of  $5^\circ$  is obtained for the pedestrian which is in line with the recommendations of the EMPIR SURFACE project<sup>7</sup> and remains close to our previous results. The mobile observer concept is implemented for observation angles greater than  $1^\circ$ .<sup>5,6,8</sup> To check that the use of this concept does not induce error, the road lighting performance criteria<sup>1-4</sup> are calculated with a mobile observer looking at  $1.43^\circ$  below the horizontal (Figures 5,6 and 7). In this way, a distance  $D$  of 60 m is maintained between the observer and the measurement point (see Equation 4), which is in line with the usual geometry of the standard observer and therefore allows a comparison.

$$\alpha = \arctan\left(\frac{H_{eyes}}{D}\right) \quad (4)$$

where  $H_{eyes}$  is the height of the observer's eyes and is equal to 1.5 m.

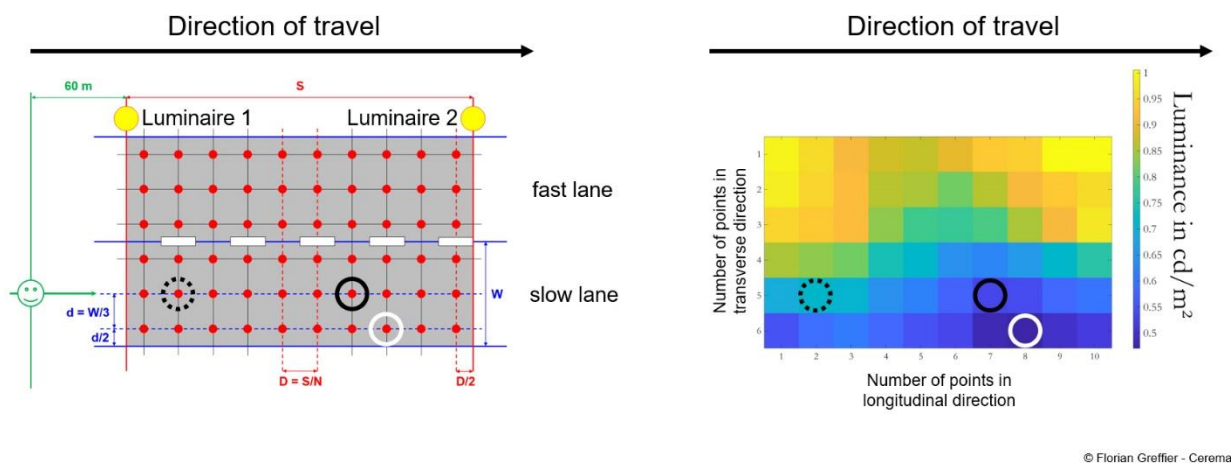
The experimental site is located on an industrial area in Limoges, France. The road is a two-lane carriageway 7 m wide, fitted with a single-sided LED lighting system with luminaires 8 m high and spaced 28.5 m apart. The road surface is an asphalt mix with a granular fraction composed of 30 % crushed porcelain (see Figure 8, left).<sup>11</sup> The photometry of the road surface was characterised by the  $r$ -tables measured with the laboratory gonioreflectometer of the Cerema<sup>6</sup> for different observation angles ( $1^\circ$ ,  $3^\circ$ ,  $5^\circ$ ,  $10^\circ$ ,  $20^\circ$ ,  $45^\circ$  and  $80^\circ$ ). The photometric solid measured for  $\alpha = 1^\circ$  is plotted in Figure 8, on the right. This road is mainly for motorised vehicles and the maximum authorised speed is 50 km/h. Given these characteristics, the lighting performance criteria of an M3 lighting class can be chosen, as is often the case in France in this type of configuration.<sup>1,12</sup> The luminous flux of the luminaires is 4766 lumens.

For each observation geometry, the horizontal illuminance, vertical illuminance at 12.5 cm from the road surface, average luminance  $L_{ave}$ , overall and longitudinal uniformities ( $U_0$  and  $U_l$ ), and Adrian's visibility level<sup>13</sup> ( $VL$ ) are calculated and measured for the slow lane only. The observer is in the middle of this lane. The  $VL$  of a 25 cm square target with 20 % reflectance is evaluated at each point on the standardised measurement grid.<sup>2,12</sup> Then, the number of visible targets in relation to the total number of target positions is calculated. A target is considered visible if its  $VL$  is greater than 7 in absolute value.<sup>14</sup> The implementation of the target visibility level calculation is explained in more detail by Lebouc.<sup>15</sup> The values of the quality criteria obtained for each observation angle in simulation and measurement are summarised in Table 2.

First of all, when we look at the classic performance criteria, there are differences between simulations and measurements, particularly in average luminance and overall uniformity. These differences were also noticed for the horizontal and vertical illuminances (not presented in this article). This may be due to parameters used in simulation that are not identical to reality, such as luminous flux of the luminaires or photometry. As these

parameters could not be verified by measurement, manufacturer's data were used. In addition, during the simulations,  $r$ -tables from a single pavement core were used. This does not take into account the heterogeneity of the road surface over the entire measurement area and could therefore explain the differences in luminance observed.<sup>6</sup>

However, despite the differences, the same trends were found. First, it appears that the standard quality criteria obtained for the standard observer at 1° and the mobile observer at 1.43° are identical. This confirms that the mobile observer can be used to assess a lighting installation with an observation angle greater than 1°.



© Florian Greffier - Cerema

**Figure 5** – Left: Normative grid ( $N = 10$  points in the longitudinal direction, 3 points per lane) for measuring and calculating the performance criteria (average luminance  $L_{ave}$ , overall uniformity  $U_0$  and longitudinal uniformity  $U_l$ ) of a lighting installation (with luminaires spaced  $S$  metres apart) for a road with two lanes (width  $W$ ) and an observer located in slow lane. Right: an example of luminance measurements in the same lighting situation.  $L_{ave}$  is the average of the 60 luminance measurements,  $U_0$  is the ratio between the minimum luminance on the grid (solid white circle) and  $U_l$  is the ratio between the minimum luminance (dotted black circle) and the maximum luminance (solid black circle) for the grid points located in the centre of the lane in which the observer is travelling.

Furthermore, the average luminance of the pavement decreases as the observation angle increases without affecting the uniformities, which is in line with the results found by Greffier *et al.*<sup>6</sup> This decrease is explained by the reduction in the reflective capacity of the pavement as the observation angle increases. As shown in Figure 8 on the right, the area of the photometric solids decreases as the observation angle increases, resulting in a decrease in  $Q_0$ <sup>16</sup> (see values in the legend to Figure 8).

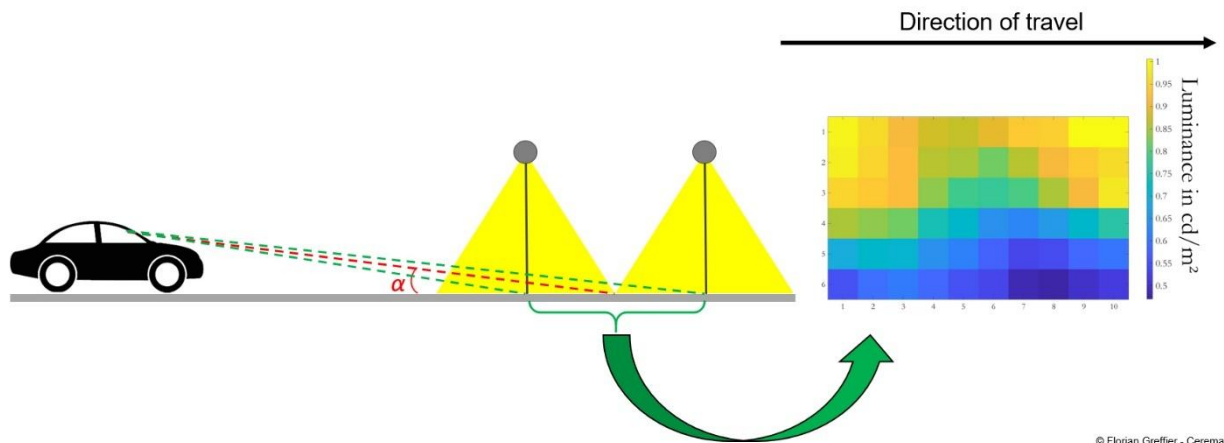


**Figure 6** – Calculation/measurement of luminance with a standard observer. The 60 grid points are calculated or measured from the same observation position.

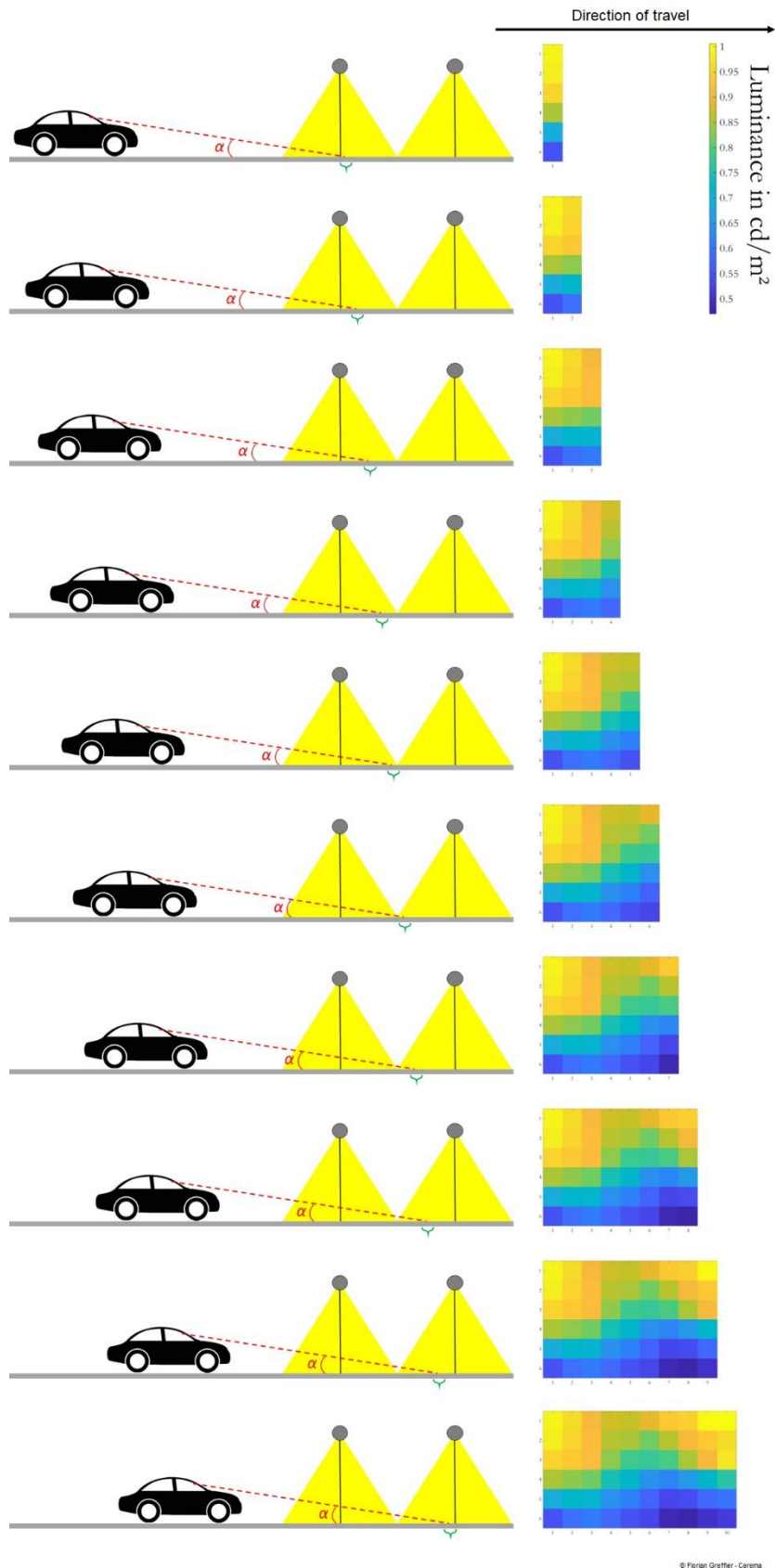


**Figure 7** – Calculation/measurement of luminance with a mobile observer. The 60 grid points are calculated or measured from successive observation positions so that the angle of observation remains the same for each grid point.

Nevertheless, the decrease in average luminance does not affect user visibility, since the percentage of visible targets does not decrease, but remains at a maximum. This can be explained by the fact that, as the observer looks closer, the apparent size of the target becomes larger.

These results show the effect of a change in geometry on the quality criteria of a lighting installation and, consequently, the need to take proper account of the users of the public space when designing it. In addition, the visibility criterion highlights the fact that lower luminance, as the angle of observation increases, is not detrimental to the visibility of users.

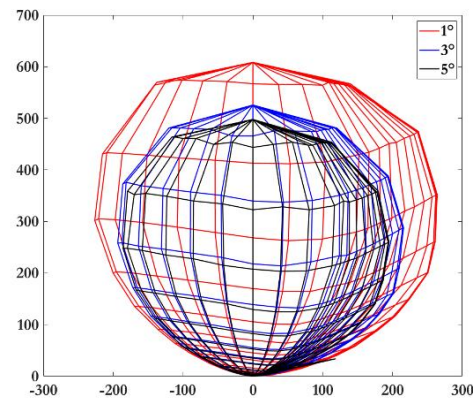
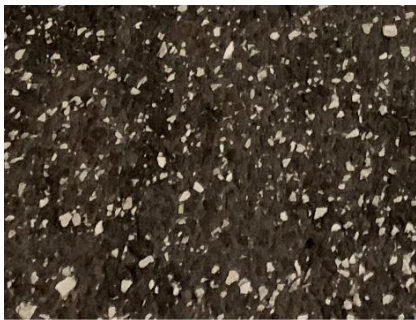


**Figure 8** – Left: Image of the surface of the road surface composed with ground porcelain. Right: Photometric solid of the same pavement for  $\alpha = 1^\circ$  ( $Q_0 = 0.110$  and  $S_1 = 0.32$ ) in red,  $\alpha = 3^\circ$  ( $Q_0 = 0.087$  and  $S_1 = 0.29$ ) in blue and  $\alpha = 5^\circ$  ( $Q_0 = 0.080$  and  $S_1 = 0.25$ ) in black.

#### 4 Adaptation of recommendations

Today, designers dimension lighting installations by considering a standard observer looking at the road surface with an observation angle of  $1^\circ$ , as recommended by the standards.<sup>2,4</sup> However, it has just been seen that an angle  $\alpha$  of  $3^\circ$  would be more appropriate for urban uses and requires lighting calculations to be implemented with a mobile observer.

However, there are two things to bear in mind. The first is that lighting designers very rarely have a  $r$ -table of the road surface and, if they do, it is measured at an observation angle of  $1^\circ$ , not  $3^\circ$ . Furthermore, lighting software does not currently offer the option of changing the observation angle. It can therefore be assumed that it is not yet possible to estimate the performance of an urban lighting installation using an angle  $\alpha$  of  $3^\circ$ . In addition, lighting designers use dimensioning software that, for the most part, they have not developed, and which therefore does not include visibility level calculations. It is therefore clear that visibility will never be assessed either, at least until practices change.

This raises the following question: how can the results presented here be useful without having able to revolutionise current practices and methodologies? Firstly, it seems necessary

to check that designing urban lighting with an angle  $\alpha$  of  $1^\circ$  would not pose a safety problem for users looking at  $3^\circ$ . Particular attention was focused on M3, M4 and M5 lighting classes because they are the most common in urban areas.

To this end, for the previous pavement/lighting combination, the luminous flux of the luminaires needed to meet the specified requirements for each lighting class is determined and visibility is assessed. Then, this same luminous flux is kept for each class and the performance obtained for a mobile observer with an angle  $\alpha$  of  $3^\circ$  are evaluated (see Table 3). The following results are based on calculations made using our own lighting software and measured  $r$ -tables at  $1^\circ$  and  $3^\circ$ .

First, the lighting class M3 is examined. The luminous flux of the luminaires is varied until an average luminance  $L_{ave} = 1.00 \text{ cd.m}^{-2}$  is obtained, with minimum uniformities  $U_0 = 0.40$  and  $U_l = 0.60$  and a maximum threshold increment  $f_{TI} = 15 \%$ . The values of the quality criteria obtained are given in Table 3. The percentage of visible targets is also evaluated, and it can be seen that this is not equal to 100 % despite the performance criteria meeting the requirements. The various criteria for a mobile observer looking at  $3^\circ$  below the horizontal are then estimated with the luminous flux previously found. First, it appears that the average luminance decreases as the angle of observation increases. This does not affect the uniformities, which remain the same. It can also be seen that the threshold increment is almost the same for  $\alpha = 1^\circ$  and  $\alpha = 3^\circ$ . Finally, for the angle of  $3^\circ$ , all the targets are considered to be visible, and when the visibility at  $3^\circ$  is compared with that obtained at  $1^\circ$ , it is found that the percentage of visible targets is higher.

The same study is done for lighting class M4. This time, the aim is to have  $L_{ave} = 0.75 \text{ cd.m}^{-2}$ ,  $U_0 = 0.40$ ,  $U_l = 0.60$  and  $f_{TI} = 15 \%$  for an observation angle of  $1^\circ$ . As with M3, there was a reduction of the average luminance. Uniformities and threshold increment were again stable. Visibility is not reduced either, since the percentage of visible targets for  $\alpha = 3^\circ$  is equal to 100 % and therefore higher than that obtained for  $\alpha = 1^\circ$ .

Finally, simulation is carried out for lighting class M5. This time, the luminous flux is adjusted to achieve  $L_{ave} = 0.50 \text{ cd.m}^{-2}$ ,  $U_0 = 0.35$ ,  $U_l = 0.40$  and  $f_{TI} = 15 \%$ . The average luminance calculated for an observer looking at  $3^\circ$  below the horizontal is again lower than that estimated for  $\alpha = 1^\circ$ . On the other hand, the uniformities and the threshold increment remained unchanged. Finally, it should be noted that the percentage of visible targets is not equal to 100 %. However, it is always higher than that found for  $1^\circ$ , which indicates that there is no loss of visibility.

These results show that, using the classic methodology ( $\alpha = 1^\circ$ ) for sizing an urban lighting installation, a lighting designer who achieves the recommended values provides sufficient visibility for users to ensure their safety, even if they are looking from an angle of  $3^\circ$ .

To go further, it has been shown that the percentage of visible targets at an observation angle of  $3^\circ$  is always greater than that determined at  $1^\circ$ . So, even though luminance at  $3^\circ$  is already decreasing, this suggests that it could perhaps be reduced even further, by lowering the luminous flux of the luminaires without penalising visibility in city. This is why, in the current context of ecological transition and therefore energy savings, a downgrading of one class for the dimensioning of lighting in town has been studied. For example, for an urban roadway categorised as M3 for observation at  $1^\circ$ , this would mean meeting the requirements of class M4 when we wish to satisfy visual needs at  $3^\circ$ .

To check if this proposal is not too optimistic, it was examined whether downgrading by one lighting class when sizing to  $1^\circ$  results in a reduction in visibility for urban uses.

First, the luminous flux is adjusted to meet the requirements of class M3 and then class M4, and the resulting performance is examined at an observation angle of  $3^\circ$ . It can be seen that the average luminance decreases but that the uniformities and the percentage of visible targets remain the same (see Table 4). The threshold increment factor is reduced by 0.5 %.

The impact of downgrading from M4 to M5 is then examined. The mean luminance changes from  $0.60 \text{ cd.m}^{-2}$  to  $0.40 \text{ cd.m}^{-2}$  and the threshold increment decreases by 0.7 %. Uniformities remain stable as before, which is not the case for visibility. Visibility is 100 % for class M4 and becomes 98 % for class M5. The percentage of visible targets obtained for class M5 with an observation angle of  $3^\circ$  is still higher than that calculated for a design meeting the requirements of class M4 with a standard observer (85 %).

Finally, the downgrading from M5 to M6 is studied. This reduces the average luminance from  $0.40 \text{ cd.m}^{-2}$  to  $0.24 \text{ cd.m}^{-2}$  without affecting uniformities. The threshold increment is also reduced. In addition, the percentage of visible targets falls by 5 %, from 98 % for the M5 class to 93 % for the M6 class. Despite this, it remains higher than the visibility obtained for class M5 with the observer looking at an  $\alpha$  angle of  $1^\circ$  (80 %).

In this section, the quality criteria obtained for the previous pavement/lighting combination are calculated with a view to proposals for lowering the required luminance levels based on maintaining visual performance. This situation confirmed that it was possible to downgrade from class M3 to class M4 without any impact on uniformities and visibility, and with a slight reduction in disability glare. It has also been shown that downgrading from M4 to M5 or from M5 to M6 can have a slight impact on visibility. However, this is at most a 5 % reduction in the percentage of visible targets. Moreover, this reduction is considered acceptable since the percentage of visible targets is still at least 10 % higher than that obtained for a conventional design according to the lower class with  $\alpha = 1^\circ$ .

Thus, based on the results obtained for this situation, it would be interesting to investigate the possibility of downgrading a class to lighting category M when designing an urban lighting

installation. We therefore plan to confirm the trends obtained by simulating the performance with other pavement/lighting combinations and by organising experiments with subjects. In this example, downgrading by one class would result in energy savings of 25 % for downgrading from M3 to M4, 33 % for M4 to M5, and 40 % for M5 to M6, compared with conventional dimensioning.

## 5 Conclusion

This paper presents an experiment conducted to find out whether the travel mode of users of urban and interurban space has an impact on the angle of observation with which they look at the road surface. For this purpose, a virtual environment representing a city and its ring road was created in Unity 3D. The participants had to move around following audio-directional instructions and concentrate on their route as in a real situation. They also had to signal the presence of an obstacle. They were given four different roles: pedestrian, cyclist, city driver and interurban motorist. The passage results of 37 participants were used for this study, which provided enough data to use for statistics.

In particular, these results show that there appears to be a significant effect of the travel mode on the distance at which the user looks. On average, a pedestrian looks closer than a car driver. In fact, as the travel speed increases, the observer looks further away in order to anticipate his or her route. Furthermore, the results indicate that the travel mode also has an effect on the dispersion of the users' observation angles. It has been noticed that the angles obtained for pedestrians are distributed over a wider range than those of motorists on interurban roads, which means that they scan more the road surface with their eyes. As a result, their attention is more dispersed and their reaction time is therefore higher.

This virtual reality experiment with subjects made it possible to define observation angles for each type of user: 1° for motorists on interurban roads, 3° for motorists in town and cyclists, 5° for pedestrians. These new observation angles were then incorporated into simulations to assess the impact of a change in observation geometry on the quality criteria of a lighting installation and a visibility criterion. Measurements were also taken on an experimental site and a comparison was made between the simulations and the measurements. It has been shown that as the angle of observation increases, the average luminance on the road decreases. However, this does not affect visibility. This result led us to propose adaptations to the current recommendations. Firstly, we agree with Stockmar<sup>8</sup> and Greffier<sup>5,6</sup> on the use of a mobile observer when the observation angle is greater than 1°. Also, the possibility of downgrading by one lighting class when dimensioning in the city in the standard way (*i.e.* with  $\alpha = 1^\circ$ ) has been studied. The results are conclusive, and we therefore plan to confirm the trends obtained by simulating the performance with other pavement/lighting combinations and by organising visibility experiments with subjects on real site. The case of pedestrians could also be explored in greater depth to show the differences between different modes of walking,



e.g. simply following the path from point A to point B, casual walking in pairs or in a group, leisurely walking while looking around frequently.

### **Conflict of interest**

The authors declare no potential conflicts of interest with respect to the research, authorship and/or publication of this paper.

### **Funding**

No funding was received for conducting this study. The authors have no relevant financial or non-financial interests to disclose.

### **Data availability statement**

The datasets generated and analysed during the current study are available from the corresponding author on reasonable request.

### **Acknowledgements**

The authors would like to thank the Plateforme Angevine d'Analyse des Comportements for the loan of the simulation equipment and especially Florian Focone for his help and expertise in setting up the experiment and simulating the virtual environment. We also thank Amélie Bret, Nathan Portier and Kévin Rolland, students at Polytech'Angers, for the development of the virtual environment. Finally, we would like to thank all the participants who kindly gave us their time.

A version of this work was also published in the Proceedings of the CIE 2023 Session

### **ORCID**

Laure Lebouc <http://orcid.org/0000-0002-4775-2651>

Florian Greffier <http://orcid.org/0000-0001-7745-6629>

Vincent Boucher <http://orcid.org/0000-0003-2299-4168>

Aurélia Nicolai <http://orcid.org/0009-0009-2152-3883>

## References

1. Comité Européen de Normalisation. *Road Lighting – Part 2: Performance requirements*. EN 13201-2:2015. Brussels, Belgium: CEN, 2015.
2. Comité Européen de Normalisation. *Road Lighting - Part 3: Calculation of Performance*. EN 13201-3:2015. Brussels, Belgium: CEN, 2015.
3. Comité Européen de Normalisation. *Road Lighting – Part 4: Methods of measuring lighting performance*. EN 13201-4:2015. Brussels, Belgium: CEN, 2015.
4. Commission Internationale de l'Éclairage. *Road Lighting Calculations, 2nd Edition*. CIE 140:2019. Vienna: CIE, 2019.
5. Greffier F, Muzet V, Boucher V, Fournela F, and Dronneau R. Use of an imaging luminance measuring device to evaluate road lighting performance at different angles of observations. *Proceedings of the 29th Quadrennial Session of the CIE*. Washington DC, USA. 14 June to 22 June, 2019: 553–562. DOI: 10.25039/x46.2019.OP75
6. Greffier F, Muzet V, Boucher V, Fournela F, and Lebouc L. Influence of Pavement Heterogeneity and Observation Angle on Lighting Design: Study with New Metrics. *Sustainability* 2021; 13: 11789.
7. Muzet V, Bernasconi J, Iacomussi P, Liandrat S, Greffier F, Blattner P, *et al.* Review of road surface photometry methods and devices – Proposal for new measurement geometries. *Lighting Research and Technology* 2020; 3(53): 213–229.
8. Stockmar A. Extension of the luminance concept in road and tunnel lighting. *Proceedings of 28th Quadrennial Session of the CIE*, Manchester, United Kingdom. 28 June to 4 July, 2015: 751–753.
9. Fotios S, Uttley J, Cheal C, Hara N. Using eye-tracking to identify pedestrians' critical visual tasks, Part 1. Dual task approach. *Lighting Research and Technology* 2015; 47(2): 133-148.
10. Field A. *Discovering Statistics Using IBM SPSS Statistics*. SAGE, 2013.
11. Carnis J. *La porcelaine, une affaire qui roule*. *Le Moniteur*. Retrieved 22 May 2024 from <https://www.lemoniteur.fr/article/la-porcelaine-une-affaire-qui-roule.594974> (in french)
12. Commission Internationale de l'Éclairage. *Lighting of Roads for Motor and Pedestrian Traffic*. CIE Publication 115:2010. Vienna: CIE, 2010.
13. Adrian W. Visibility of Targets: Model for Calculation. *Lighting Research and Technology* 1989; 21: 181-188.

14. Lecocq J. Visibility levels in outdoor lighting: Adrian model applied to spherical cap targets. *Proceedings of the 22th session of the CIE*, Melbourne, Australia. 1991: 48–51.
15. Lebouc L, Boucher V, Greffier F, Liandrat S, Nicolai A, and Richard P. Influence of road surfaces on the calculation of a target visibility taking into account the direct and indirect lighting. *CIE 2021 Midterm Meeting and Conference*, Kuala Lumpur, Malaysia (*online*). 27 September to 29 September, 2021: 32–41. DOI: 10.25039/x48.2021.OP03
16. Commission Internationale de l'Éclairage. *Road surface and road marking reflection characteristics*. CIE 144:2001. Vienna: CIE, 2001.

**Table 1 – Significant values about angles and reaction times for each travel mode.**

Travel mode	Pedestrian (6 km/h)	Cyclist (12 km/h)	Motorist in town (25 km/h)	Motorist on interurban road (75 km/h)
Average observation angle ( $\alpha_{mean}$ )	4.2°	3.1°	2.9°	1.0°
Standard deviation of the observation angle ( $\sigma$ )	2.9°	1.8°	1.5°	0.5°
Distance in the road plane ( $D$ )	20.4 m	27.7 m	29.6 m	85.9 m
Average reaction time	840 ms	715 ms	668 ms	544 ms
Standard deviation of reaction time	567 ms	372 ms	334 ms	165 ms

**Table 2 – Quality criteria calculated (in blue) and measured (in orange) on the slow lane for different observation geometries using a standard observer for values at 1° and a mobile observer for values at 1.43°, 3° and 5°.**

Angle $\alpha$	$L_{ave}$ (in cd.m <sup>-2</sup> )		$U_0$		$U_l$		$ VL  > 7$	
1°	1.22	1.16	0.78	0.63	0.72	0.76	100 %	100 %
1.43°	1.22	1.07	0.78	0.62	0.72	0.74	100 %	100 %
3°	0.98	0.86	0.76	0.60	0.71	0.72	100 %	100 %
5°	0.89	0.69	0.74	0.65	0.71	0.73	100 %	100 %

**Table 3 – Simulation results for different lighting classes considering the lighting installation and pavement on the experimental site.**

M3	Luminous flux: 5000 lumens	$\alpha$	$L_{ave}$ (in $\text{cd.m}^{-2}$ )	$U_0$	$U_l$	$f_{TI}$ (in %)	$ VL  > 7$
		1°	1.00	0.44	0.72	9.6	87 %
		3°	0.80	0.43	0.71	9.3	100 %
M4	Luminous flux: 3750 lumens	$\alpha$	$L_{ave}$ (in $\text{cd.m}^{-2}$ )	$U_0$	$U_l$	$f_{TI}$ (in %)	$ VL  > 7$
		1°	0.75	0.44	0.72	9.1	85 %
		3°	0.60	0.43	0.71	8.8	100 %
M5	Luminous flux: 2500 lumens	$\alpha$	$L_{ave}$ (in $\text{cd.m}^{-2}$ )	$U_0$	$U_l$	$f_{TI}$ (in %)	$ VL  > 7$
		1°	0.50	0.44	0.72	8.3	80 %
		3°	0.40	0.43	0.71	8.1	98 %

**Table 4 – Simulation results for different lighting classes considering the lighting installation and pavement on the experimental site.**

M3	Luminous flux: 5000 lumens	$\alpha$	$L_{ave}$ (in $\text{cd.m}^{-2}$ )	$U_0$	$U_l$	$f_{TI}$ (in %)	$ VL  > 7$
		1°	1.00	0.44	0.72	9.6	87 %
		3°	0.80	0.43	0.71	9.3	100 %
M4	Luminous flux: 3750 lumens	$\alpha$	$L_{ave}$ (in $\text{cd.m}^{-2}$ )	$U_0$	$U_l$	$f_{TI}$ (in %)	$ VL  > 7$
		1°	0.75	0.44	0.72	9.1	85 %
		3°	0.60	0.43	0.71	8.8	100 %
M5	Luminous flux: 2500 lumens	$\alpha$	$L_{ave}$ (in $\text{cd.m}^{-2}$ )	$U_0$	$U_l$	$f_{TI}$ (in %)	$ VL  > 7$
		1°	0.50	0.44	0.72	8.3	80 %
		3°	0.40	0.43	0.71	8.1	98 %
M6	Luminous flux: 1500 lumens	$\alpha$	$L_{ave}$ (in $\text{cd.m}^{-2}$ )	$U_0$	$U_l$	$f_{TI}$ (in %)	$ VL  > 7$
		1°	0.30	0.44	0.72	7.5	68 %
		3°	0.24	0.43	0.71	7.3	93 %